Non-Debye relaxation in the dielectric response of nematic liquid crystals: Surface and memory effects in the adsorption-desorption process of ionic impurities

J. L. de Paula,[1] P. A. Santoro,[1] R. S. Zola,[1] E. K. Lenzi,[1] L. R. Evangelista,[1] F. Ciuchi,[2] A. Mazzulla,[2] and N. Scaramuzza[2,3]

[1]*Departamento di Física, Universidade Estadual de Maringá, Avenida Colombo 5790, 87020-900 Maringá, Paraná, Brazil*

[2]*CNR-IPCF UoS di Cosenza, Licryl Laboratory, and Centro di Eccellenza CEMIF.CAL Università della Calabria, 87036 Arcavacata di Rende, Italy*

[3]*Dipartimento di Fisica, Università della Calabria, 87036 Arcavacata di Rende, Italy*

(Received 25 July 2012; published 26 November 2012)

We demonstrate theoretically that the presence of ions in insulating materials such as nematic liquid crystals may be responsible for the dielectric spectroscopy behavior observed experimentally. It is shown that, at low frequencies, an essentially non-Debye relaxation process takes place due to surface effects. This is accomplished by investigating the effects of the adsorption-desorption process on the electrical response of an electrolytic cell when the generation and recombination of ions is present. The adsorption-desorption is governed by a non-usual kinetic equation in order to incorporate memory effects related to a non-Debye relaxation and the roughness of the surface. The analysis is carried out by searching for solutions to the drift-diffusion equation that satisfy the Poisson equation relating the effective electric field to the net charge density. We also discuss the effect of the mobility of the ions, i.e., situations with equal and different diffusion coefficients for positive and negative ions, on the impedance and obtain an exact expression for the admittance. The model is compared with experimental results measured for the impedance of a nematic liquid crystal sample and a very good agreement is obtained.

DOI: 10.1103/PhysRevE.86.051705 PACS number(s): 83.80.Xz, 82.45.−h

I. INTRODUCTION

Dielectric spectroscopy is widely used for characterizing the molecular dynamics of various systems, including fuel cells [1] and biological tissues [2]. In liquid crystals, this is an important technique because it provides information about the various molecular relaxation modes associated with molecular rotation [3]. Moreover, it also provides information about the conductivity and the permittivity, which are particularly important for display applications. Nevertheless, liquid crystals are insulating materials, and their finite resistance comes from the ionic impurities dissolved in the medium. In fact, ionic charges represent an essential contribution for the dielectric properties of liquid crystals, since the small quantity of impurities is difficult to eliminate [3]. In displays, these ions change the resistance of the material and challenge the industry to avoid phenomena such as low VHR (voltage holding ratio) and image sticking [3,4]. When an insulated material is submitted to an alternating current, the presence of ions will play a decisive role in the electrical impedance of the material, especially at low frequencies, where the time scales involved allow for strong surface effects, such as the adsorption-desorption phenomenon. These effects may be responsible for a non-Markovian comportment of the stochastic processes, i.e., an anomalous behavior. Several mechanisms may lead to a non-usual behavior of the system such as memory effects [5,6], long-range interactions [7–9], long-range correlations [10], and surface effects [11–15]. The last point plays an important role [16,17] in understanding the dynamic aspects of the ions on the electrical response of liquid crystals and their applications in several contexts. In this sense, different mechanisms have been proposed to explain the dynamic of ions in these materials such as the dissociation of neutral particles into ionic products, the recombination of these ions giving rise to neutral particles [18–28], electrodes with fractal interfaces [29–31], the adsorption-desorption process occurring at the interfaces [28,32–34], and extensions based on fractional diffusion equations [35–42] connected to anomalous diffusion. Here, we consider an electrolytic cell such as liquid crystals in the framework of the Poisson-Nernst-Planck model, taking into account the dissociation-association process. The surface contribution is accounted for by means of a general kinetic equation representing the adsorption-desorption processes occurring at the interfaces. By using this general equation, we extend the usual discussed in Ref. [43] which is characterized by a relaxation regime with a non-usual (or non-Debye) relaxation. As we will show below, this equation contains a fractional time derivative and a temporal kernel associated with the desorption rate that may be connected to memory effects, as discussed in Refs. [12,13]. Indeed, in the adsorption of ions at a solid electrode, an elastic scattering occurs when there is no loss of translational energy during the collision; however, if the ion is still in a weakly bound state, even if it is on the surface, the thermal motion of the surface atoms can cause the ion to desorb. Finally, when the ion collides with a surface, it loses energy and is converted into a state where it remains on the surface for a reasonable time, i.e., it is physically adsorbed. As a consequence, the actual position of the ion on the electrode has a memory of its incoming state, eventually modifying the adsorption-desorption rates. These effects may also be connected to the roughness of the surface, which in the low-frequency limit leads us to obtain $Y = 1/Z \propto (i\omega)^{\overline{\eta}}$ where Y and Z denote the admittance and the impedance and $\overline{\eta}$ is a parameter connected to the roughness of the surface [44,45] (see also Refs. [46,47] for an additional discussion). The solution of the problem in the absence of the adsorption-desorption process has been presented in Refs. [19,48], and the solution without generation and recombination of ions can be found in Refs. [32–34]. The mathematical problem is faced by means of analytical methods, and the solutions are found by assuming first that

the diffusion coefficients of the positive and negative ions are different, which constitutes a more appropriate scenario for describing the impedance response of insulating materials such as liquid crystals. The non-Debye relaxation process can be used for explaining non-usual behavior observed in bent-core liquid crystal [49] and nematic cells with strong dipoles (e.g., materials with cyano groups such as the *n* CB family) [50].

The paper is organized as follows: Sec. II presents the fundamental equations relevant to the drift-diffusion problem for ions in an insulating medium, in the presence of the generation-recombination phenomenon, described as a first-order chemical reaction, and incorporating a generalized kinetic equation at the interface. The case in which the neutral particles are trapped and the positive and negative ions have different mobilities is discussed in Sec. III, where it is shown that the adsorption-desorption phenomenon is responsible for a low-frequency plateau in the real part of the electrical impedance. Theoretical predictions and a comparison with experimental data are presented in Sec. IV. Concluding remarks are drawn in Sec. V.

II. CONTINUOUS MODEL

Consider a slab of thickness d, whose electrodes are placed at $z = \pm d/2$, with z the axis normal to the surfaces. In addition to the situation treated in Ref. [48], where the sample has the same geometry, in the present approach the adsorption-desorption process is incorporated at the surface of the electrodes and governed by a non-usual kinetic equation that can be connected to a non-Debye relaxation, as shown below.

A. Kinetic equation

We denote by N_n, N_p, and N_m the bulk densities of neutral, positive, and negative particles, respectively. The equations of continuity, stating the conservation of particles, are

$$\frac{\partial}{\partial t}N_n = -\frac{\partial}{\partial z}J_n - c_d N_n + c_a N_p N_m \quad \text{and} \tag{1}$$

$$\frac{\partial}{\partial t}N_\alpha = -\frac{\partial}{\partial z}J_\alpha + c_d N_n - c_a N_p N_m, \tag{2}$$

with the bulk densities of current of particles being given, respectively, by

$$J_n = -D_n\frac{\partial}{\partial z}N_n\,, \quad \text{and} \tag{3}$$

$$J_\alpha = -D_\alpha\left[\frac{\partial}{\partial z}N_\alpha + \frac{q}{k_B T}N_\alpha\frac{\partial}{\partial z}V\right], \tag{4}$$

where $V(z,t)$ is the electrical potential, q is the ion charge, k_B is the Boltzmann constant, T is the absolute temperature, and α refers to either the positive ion ($\alpha = p$) or the negative ion ($\alpha = m$). In the preceding equations, c_a and c_d are, respectively, the constants of association and dissociation. The corresponding diffusion coefficients for the two types of ions are D_p and D_m, with D_n being the diffusion coefficient for neutral particles.

The next step in the construction of the continuous model is to invoke the Poisson equation governing the bulk density of charges, $\rho(z,t) = q(N_p - N_m)$, simply written in the form

$$\frac{\partial^2}{\partial z^2}V(z,t) = -\frac{q}{\varepsilon}(N_p - N_m), \tag{5}$$

where ε is the dielectric constant of the medium. Thus, the complete mathematical problem consists in solving the set of Eqs. (1)–(5), satisfying the boundary conditions

$$J_n\left(\pm\frac{d}{2},t\right) = 0, \tag{6}$$

$$J_\alpha(z,t)\Big|_{z=\pm\frac{d}{2}} = \pm\frac{d}{dt}\sigma_\alpha(t), \tag{7}$$

$$V\left(\pm\frac{d}{2},t\right) = V_0\left(\pm\frac{d}{2},t\right), \tag{8}$$

which state that the electrodes are blocking for neutral particles (6). The adsorption-desorption phenomenon, governed by the general kinetic equation

$$\tau^\gamma\frac{d^\gamma}{dt^\gamma}\sigma_\alpha(t) = \kappa\tau\, N_\alpha\left(\pm\frac{d}{2},t\right) - \int_{-\infty}^{t} d\bar{t}\,K(t-\bar{t})\sigma_\alpha(\bar{t}), \tag{9}$$

is now imposed for the mobile ions (7), and the bulk electrical potential profile on the surface always coincides with the applied potential (8). In Eq. (9), the fractional operator is the Caputo one [51], defined as

$$\frac{d^\gamma}{dt^\gamma}\sigma_\alpha(t) = \frac{1}{\Gamma(n-\gamma)}\int_0^t \frac{\sigma_\alpha^{(n)}(t')}{(t-t')^{\gamma+1-n}}\,dt', \quad n-1<\gamma<n, \tag{10}$$

which reduces to the usual derivative if $\gamma = n$, with n an integer and non-negative. The problem as formulated above is a further generalization of the problem treated in Ref. [28], in which a usual kinetic equation describing a chemical reaction of the first species was considered. The developments based on the usual kinetic equation of the first species has a correspondence with the theory presented by Macdonald and Franceschetti in Ref. [19]. This pioneer approach adopts Chang-Jaffe boundary conditions to take specific adsorption at the electrodes into account. In this direction, a similar approach was recently proposed in terms of an usual kinetic equation at the interfaces (Langmuir's approximation) to get some details about the role of the adsorption-desorption process in combination with the phenomenon of ionic recombination [28]. In the kinetic equation, Eq. (9), κ and τ are parameters describing the adsorption phenomenon in such a way that $\kappa\tau$ has the dimension of length. It can be interpreted as the characteristic length over which the adsorption-desorption phenomenon takes place in the sample. This kind of approach is thus characterized by the presence of three characteristic lengths, namely, the Debye screening length (to be introduced later in the formalism), the thickness of the sample d, and this intrinsic length, giving an idea of the spatial extension involved in the adsorption process for each type of ion α. Furthermore, the kernel $K_\alpha(t)$ is connected to the effect of the surfaces on the bulk. In particular, the kernel is present in the desorption term, accounting for memory effects that may be connected to the roughness of the surface electrode in the process. In fact, as discussed in Ref. [44], the surface roughness plays an important role in determining the anomalous character of the impedance. It is therefore expected that this effect, as

shown in Refs. [12,13,44], may lead to a non-usual relaxation and, consequently, to an anomalous diffusion. This approach, based on a generalized kinetic equation, is investigated in the context of charged particles to analyze the stationary solution, in contrast to the results presented before [11–14], which were obtained for neutral particles as an initial problem of boundary condition. Another aspect to be underlined in this regard is that the results obtained here, with Eq. (9), differently from the ones presented, for example, in Refs. [17,28], come from a much more general problem, where non-Debye, hence more realistic, surface effects are considered to represent the behavior in the low-frequency limit, governed by a power law equation, i.e., $\mathcal{Z} \sim 1/(i\omega)^{\overline{\gamma}}$, where $\overline{\gamma} < 1$ is a parameter describing the behavior of the impedance. This behavior is essential to describe a wide variety of experimental data as, for example, ionic solutions and liquid crystals. The lack of an equation such as Eq. (9) cannot describe any complex, low-frequency surface effect whatsoever. Such an aspect of the experimental data cannot be accounted for by using the formalism discussed in Refs. [17,28], where usual kinetic equations are employed to incorporate adsorption effects.

B. Linear approximation

As in preceding works [32,48], the analysis is limited to the linear approximation. The applied potential has the form $V_0(\pm d/2,t) = \pm(V_0/2)\exp(i\omega t)$, where V_0 is the amplitude and ω is the circular frequency of the applied voltage. We assume that for low-amplitude V_0, it is possible to write $N_n = \overline{N}_n + \delta n_n$, $N_p = \overline{N} + \delta n_p$, and $N_m = \overline{N} + \delta n_m$ and to work in the limit $\overline{N}_n \gg \delta n_n$, $\overline{N} \gg \delta n_p$, and $\overline{N} \gg \delta n_m$, which states that, in the low-voltage regime, the densities differ only slightly from the zero field densities, where the over line symbols represent the charged particles in the bulk. Similar assumptions are made for the adsorbed quantities, which become $\sigma_p = \sigma + \delta s_p \approx \sigma$ and $\sigma_m = \sigma + \delta s_m \approx \sigma$, because $\sigma \gg \delta s_p$ and $\sigma \gg \delta s_m$. In particular, one can write $N_0 = N + \overline{N}_n$ (where N_0 represents the bulk dissociable particles plus adsorbed particles by the surface) and $c_d N_n = c_a \overline{N}^2$, with $\overline{N} = N/[1 + 2\kappa\tau/(d\overline{K})]$ and $\sigma = \kappa\tau N/[\overline{K} + 2\kappa\tau/d]$, where $\overline{K}_\alpha = \int_0^\infty K_\alpha(u)du$ and it is assumed, henceforth, that $K_\alpha(t) = K(t)$. Since the electrodes are not blocking for charged particles, the total number of mobile charges in the bulk fluctuates. For this reason, it is necessary to impose the conservation of the number of particles, which takes the simple form $\delta s_p + \delta s_m + \int_{-d/2}^{d/2}[\delta n_n + (\delta n_p + \delta n_m)/2]dz = 0$.

In the limit of low applied voltage, the solutions of the problem can be sought in the form

$$\begin{aligned} \delta n_\alpha(z,t) &= \eta_\alpha(z)e^{i\omega t}, \quad \text{with} \quad \alpha = n,p,m, \\ \delta s_\alpha(t) &= \sigma_\alpha e^{i\omega t}, \quad \text{and} \\ V(z,t) &= \phi(z)e^{i\omega t}, \end{aligned} \tag{11}$$

which permits the rewriting the fundamental equations of the problem as

$$i\omega\eta_n = D_n\frac{d^2}{dz^2}\eta_n - c_d\eta_n + c_a\overline{N}(\eta_p + \eta_m), \tag{12}$$

$$i\omega\eta_\alpha = D_\alpha\frac{d^2}{dz^2}\eta_\alpha + \frac{q\overline{N}}{k_BT}D_\alpha\frac{d^2}{dz^2}\phi + c_d\eta_n - c_a\overline{N}(\eta_p + \eta_m), \tag{13}$$

$$\frac{d^2}{dz^2}\phi = -\frac{q}{\varepsilon}(\eta_p - \eta_m). \tag{14}$$

Equations (12)–(14) have to be solved with the boundary conditions

$$D_n\frac{d}{dz}\eta_n\Big|_{z=\pm\frac{d}{2}} = 0, \tag{15}$$

$$-\left(D_\alpha\frac{d}{dz}\eta_\alpha \pm \frac{q\overline{N}}{k_BT}D_\alpha\frac{d}{dz}\phi\right)\Big|_{z=\pm\frac{d}{2}} = \pm i\omega\sigma_\alpha, \tag{16}$$

$$\phi\left(\pm\frac{d}{2}\right) = \pm\frac{V_0}{2}, \tag{17}$$

where

$$\begin{aligned} \sigma_\alpha &= \frac{\kappa\tau\eta_\alpha}{(i\omega\tau)^\gamma + K(i\omega)}\Big|_{z=\pm d/2}, \\ K(i\omega) &= e^{-i\omega t}\int_{-\infty}^{t} d\bar{t}e^{i\omega\bar{t}}K(t-\bar{t}). \end{aligned} \tag{18}$$

This completes the mathematical formulation of the problem in the linear approximation, which is usually employed when the amplitude of the applied voltage can be considered small enough. Notice the generality of the problem in considering three different mobile particles with different mobilities when the adsorption-desorption phenomenon is taken into account by means of a fractional kinetic equation combined with the effects of association-dissociation of particles in the system. Several situations of experimental relevance can be analyzed in this general framework because, as shown below, we were able to analytically solve this difficult mathematical problem. In the following, for simplicity and to compare the predictions and results with experimental data, we discuss the particular case $D_p \neq D_m$ with $D_n = 0$, which is relevant to describe a typical electrolytic cell.

III. IMMITTANCE RESPONSE OF THE CELL—EXACT RESULTS

As stated before, the mathematical problem formulated in the preceding sections can be analytically solved for $D_p \neq D_m$ with $D_n = 0$. Indeed, the solutions of the set of Eqs. (12)–(14) are given by

$$\eta_p = C_p^{(1)}e^{\gamma_1 z} + C_p^{(2)}e^{-\gamma_1 z} + C_p^{(3)}e^{\gamma_2 z} + C_p^{(4)}e^{-\gamma_2 z}, \tag{19}$$

$$\eta_m = C_m^{(1)}e^{\gamma_1 z} + C_m^{(2)}e^{-\gamma_1 z} + C_m^{(3)}e^{\gamma_2 z} + C_m^{(4)}e^{-\gamma_2 z}, \tag{20}$$

with

$$\frac{C_m^{(1)}}{C_p^{(1)}} = \frac{C_m^{(2)}}{C_p^{(2)}} = -\frac{1}{\lambda_p}\left(\gamma_1^2 - \xi_p^2\right) = k_1, \tag{21}$$

$$\frac{C_m^{(3)}}{C_p^{(3)}} = \frac{C_m^{(4)}}{C_p^{(4)}} = -\frac{1}{\lambda_p}\left(\gamma_2^2 - \xi_p^2\right) = k_2, \tag{22}$$

where k_1 and k_2 are constants and

$$\gamma_{1,2} = \sqrt{\tfrac{1}{2}(\xi_{pm}) \pm \tfrac{1}{2}\sqrt{(\xi_{pm})^2 - 4\left(\xi_p^2\xi_m^2 - \beta_p\beta_m\right)}}, \tag{23}$$

where $\xi_{pm} = \xi_p^2 + \xi_m^2$ and with

$$\xi_\alpha^2 = \frac{1}{2\lambda^2} + \frac{i\omega c_a \overline{N}}{(c_d + i\omega)D_\alpha} + \frac{i\omega}{D_\alpha} \quad \text{and}$$
$$\beta_\alpha = \frac{1}{2\lambda^2} - \frac{i\omega c_a \overline{N}}{(c_d + i\omega)D_\alpha}, \tag{24}$$

where $\lambda = \sqrt{\varepsilon k_B T/(2\overline{N}q^2)}$ is the Debye screening length. By using the previous equations, from Eq. (14) it is possible to show that the potential for this system is given by

$$\phi(z) = -\frac{q}{\varepsilon}\left\{\frac{1-k_1}{\gamma_1^2}\left(C_p^{(1)}e^{\gamma_1 z} + C_p^{(2)}e^{-\gamma_1 z}\right) + \frac{1-k_2}{\gamma_2^2}\left(C_p^{(3)}e^{\gamma_2 z} + C_p^{(4)}e^{-\gamma_2 z}\right)\right\} + Az + B\,. \tag{25}$$

Equations (19), (20), and (25) may also be simplified by applying the condition $\phi(z) = -\phi(-z)$. Thus,

$$\eta_p = 2C_p^{(1)}\sinh(\gamma_1 z) + 2C_p^{(3)}\sinh(\gamma_2 z), \tag{26}$$

$$\eta_m = 2k_1 C_p^{(1)}\sinh(\gamma_1 z) + 2k_2 C_p^{(3)}\sinh(\gamma_2 z), \tag{27}$$

$$\phi(z) = -\frac{q}{\varepsilon}2\left\{\frac{1-k_1}{\gamma_1^2}C_p^{(1)}\sinh(\gamma_1 z) + \frac{1-k_2}{\gamma_2^2}C_p^{(3)}\sinh(\gamma_2 z)\right\} + Az\,. \tag{28}$$

In order to obtain a relation between $C_p^{(1)}$ and $C_p^{(3)}$, Eqs. (16) and (17) can be used, yielding

$$C_p^{(3)} = -\Lambda C_p^{(1)}, \tag{29}$$

with

$$\Lambda(i\omega) = \frac{(1+k_1)\gamma_1\cosh(\gamma_1 d/2) + i\omega[G_p(i\omega) + k_1 G_m(i\omega)]\sinh(\gamma_1 d/2)}{(1+k_2)\gamma_2\cosh(\gamma_1 d/2) + i\omega[G_p(i\omega) + k_2 G_m(i\omega)]\sinh(\gamma_2 d/2)}, \tag{30}$$

where $G_\alpha(i\omega) = \kappa\tau/\{[(i\omega\tau)^\gamma + K(i\omega)]D_\alpha\}$. By using Eq. (29) and the boundary conditions Eqs. (15)–(17), it is possible to show that

$$A = -\frac{4\lambda^2 q}{\varepsilon}F_1(i\omega)C_p^{(1)} \quad \text{and}$$
$$\frac{C_p^{(1)}}{V_0} = -\frac{\varepsilon}{4\lambda^2 q}\frac{1}{\Delta(i\omega) + F_1(i\omega)d}, \tag{31}$$

where

$$F_1(i\omega) = \left[\left(\gamma_1 - \frac{1-k_1}{2\gamma_1\lambda^2}\right)\cosh\left(\gamma_1\frac{d}{2}\right) - \left(\gamma_2 - \frac{1-k_2}{2\gamma_2\lambda^2}\right)\Lambda(i\omega)\cosh\left(\gamma_2\frac{d}{2}\right)\right] + i\omega G_p(i\omega)\left[\sinh\left(\gamma_1\frac{d}{2}\right) - \Lambda(i\omega)\sinh\left(\gamma_2\frac{d}{2}\right)\right] \tag{32}$$

and

$$\Delta(i\omega) = \frac{1-k_1}{\gamma_1^2\lambda^2}\sinh\left(\gamma_1\frac{d}{2}\right) - \frac{1-k_2}{\gamma_2^2\lambda^2}\Lambda(i\omega)\sinh\left(\gamma_2\frac{d}{2}\right). \tag{33}$$

The electric field can be obtained from Eq. (11) as $E(z,t) = -\partial V(z,t)/\partial z$. Thus, the electrical current will be given as $I = Sd\Sigma/dt$, where S is the electrode surface and Σ is the surface density of charge on the electrode at $z = d/2$, being determined by the value of the field at the surface, i.e., $E(d/2,t) = -[\Sigma(t) + q\sigma(t)]/\varepsilon$, with $q\sigma = (\sigma_p - \sigma_m)q$ expressing the net adsorbed charge at $z = d/2$. By using these quantities, the admittance $Y = I/V$ and, consequently, the impedance $Z = 1/Y$ of the system can be easily determined. Thus, combining all the results reported above, one finally has

$$Y = \frac{i\omega\varepsilon S}{2\lambda^2}\frac{F_2(i\omega) + 2\lambda^2 F_1(i\omega)}{\Delta(i\omega) + dF_1(i\omega)}, \tag{34}$$

where

$$F_2(i\omega) = (1-k_1)[\cosh(\gamma_1 d/2)/\gamma_1 + \sinh(\gamma_1 d/2)] - (1-k_2)[\cosh(\gamma_2 d/2)/\gamma_2 - \sinh(\gamma_2 d/2)]\Lambda(i\omega)\,.$$

IV. RESULTS

A. Theoretical predictions

Let us now highlight some of the main predictions of the model worked out before. Figure 1(a) shows the behavior of the real part of the impedance for different values of the diffusion coefficients when the adsorption-desorption process is characterized by Eq. (9), with the kernel $K(t) = \delta(t/\tau)/\tau$ and $\gamma = 1$, which corresponds to a Debye relaxation, i.e., the usual kinetic equation. The generation and recombination of ions are also considered in Fig 1(a). In this figure, the dashed curve represents the case where generation-recombination and adsorption-desorption are not considered and the positive and negative ions are assumed to have equal mobilities. The dotted curves represent the same conditions as the dashed curves, except that the diffusion coefficients have different values. In both cases, the impedance assumes a constant value for low frequencies. The squares show the case where the diffusion coefficients are different and the combination-recombination effect is not present. In this case, the two phenomena interplay, and two different behaviors, represented by two different plateaus, are observed, indicating that the two phenomena occur at different time scales. Finally, the circles and the solid line represent the situation where the adsorption-desorption effect is present. The solid line was depicted for the case where the combination-recombination effect is not present,

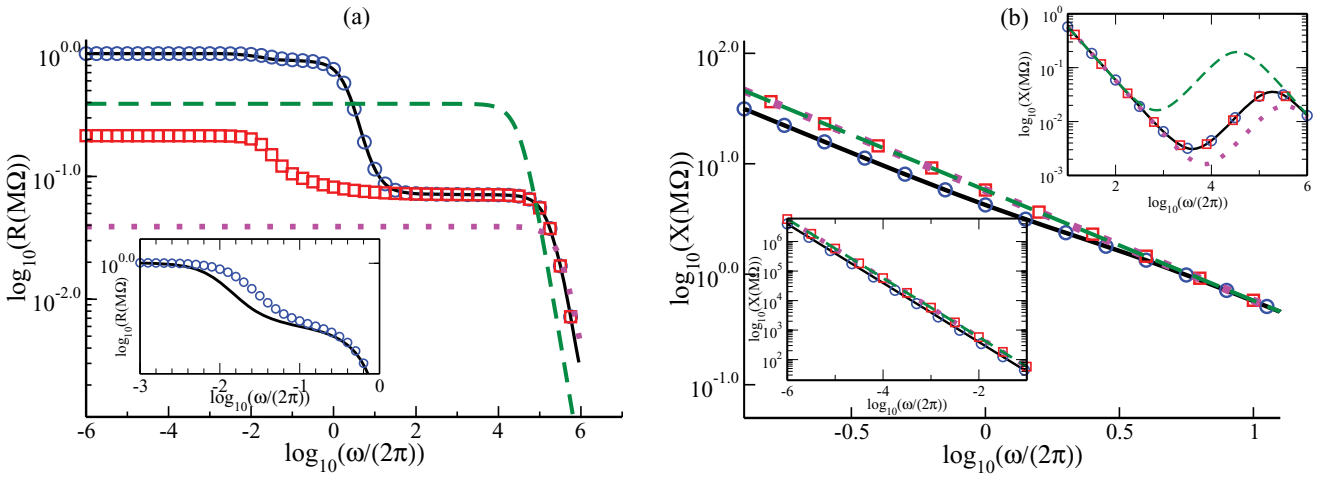

FIG. 1. (Color online) Illustration of the real (a) and imaginary (b) parts of the impedance vs $\log[\omega/(2\pi)]$. The circles correspond to the case characterized by $D_p = 10^{-7}$ m^2/s, $D_m = 10^{-8}$ m^2/s, $c_d = 10\,\mathrm{s}^{-1}$, $c_a = 5 \times 10^{-20}$ m^3/s, $\sigma_p = \sigma_m = 10^{-6}$, and $\tau = 0.1$ s. The solid line (black) represents the effect of adsorption-desorption by taking into account the parameters used for the circles (blue) in the absence of association-dissociation. The squares (red) show only the effect of different ionic mobility on the real part of the impedance. The dashed (green) and dotted (pink) lines illustrate the usual case for $D_p = D_m = 10^{-7}$ m^2/s and $D_p = D_m = 10^{-8}$ m^2/s, respectively, in absence of adsorption-desorption or association-dissociation of ions. For simplicity, the other parameters used were $S = 2 \times 10^{-4}$ m^2, $d = 10^{-3}$ m, $\lambda = 2.15 \times 10^{-7}$ m, and $\epsilon = 6.7\epsilon_0$. The inset in (a) displays a zoom in the region $-3 \leqslant \log_{10}(\omega/(2\pi)) \leqslant 0$, showing the small contribution of combination-recombination when adsorption-desorption is present. In (b), for clarity, the main frame displays the region $-1 \leqslant \log_{10}(\omega/(2\pi)) \leqslant 1$. The bottom left corner inset presents the region $-6 \leqslant \log_{10}(\omega/(2\pi)) \leqslant -1$, while the top right corner inset shows the region $1 \leqslant \log_{10}(\omega/(2\pi)) \leqslant 6$.

whereas the circles refer to the most general case. It is clear that the adsorption-desorption effect is the dominant one in the low-frequency regime, where the time scales involved dictates the strong interaction with the surfaces. The inset exhibits a zoom in the region $(-3 \leqslant \log_{10}[\omega/(2\pi)] \leqslant 0)$, showing the small contribution of the combination-recombination process when the adsorption-desorption phenomenon is present.

Figure 1(b) shows the imaginary part of the impedance, using the same parameters as in Fig. 1(a). For the imaginary part of the impedance, in this context, it is verified that the adsorption-desorption and the generation-recombination phenomena of ions are influential in the low and intermediate frequencies regime. In the high frequency regime, the standard behavior is verified, which is obtained when blocking electrodes are considered. In Fig 1(b), for clarity, the main frame displays the region $-1 \leqslant \log_{10}(\omega/(2\pi)) \leqslant 1$. The bottom left corner inset presents the region $-6 \leqslant \log_{10}(\omega/(2\pi)) \leqslant -1$, while the top right corner inset shows the region $1 \leqslant \log_{10}(\omega/(2\pi)) \leqslant 6$.

In Fig. 2, the kernel $K(t) = \delta(t/\tau)/\tau - \mathcal{K}_1(\tau/t)^{1+n}e^{-\tau/t}/\tau$ is considered, with $n = 1/2$, $\mathcal{K}_1 = 1/\Gamma(n)$, and $\gamma \neq 1$, which presents a non-usual relaxation for short times and for long

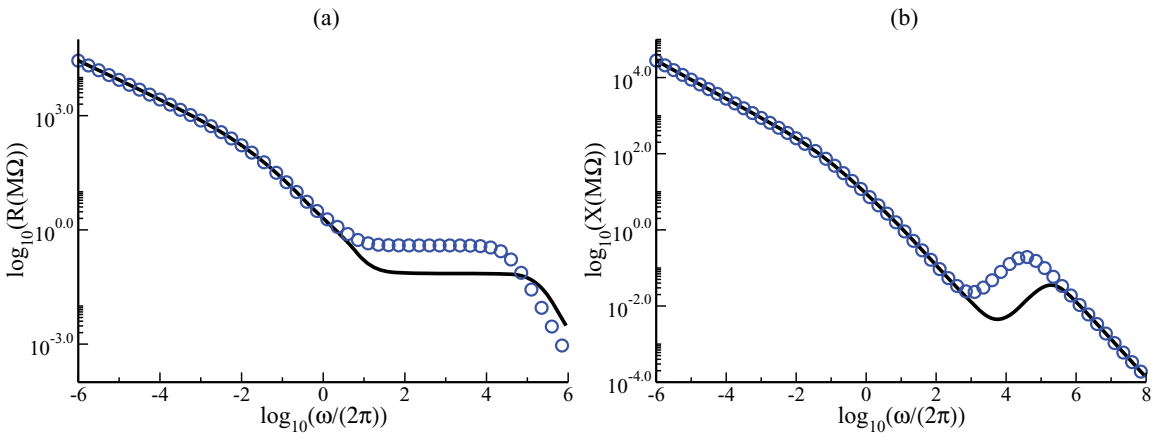

FIG. 2. (Color online) Illustration of the real (R) and imaginary (X) parts of the impedance vs $\log(\omega/(2\pi))$. The solid line (black) corresponds to the case characterized by $D_p = 10^{-7}$ m^2/s, $D_m = 10^{-8}$ m^2/s, $c_d = 10\,\mathrm{s}^{-1}$, $c_a = 5 \times 10^{-20}$ m^3/s, $\sigma_p = \sigma_m = 10^{-6}$, and $\tau = 0.1$ s. The circles (blue) show the effect of the adsorption-desorption by taking into account the parameters used for the solid line with $D_p = D_m = 10^{-8}$ m^2/s in the absence of association-dissociation. For these cases, it is also considered, for simplicity, $S = 2 \times 10^{-4}$ m^2, $d = 10^{-3}$ m, $\lambda = 2.15 \times 10^{-7}$ m, and $\varepsilon = 6.7\varepsilon_0$.

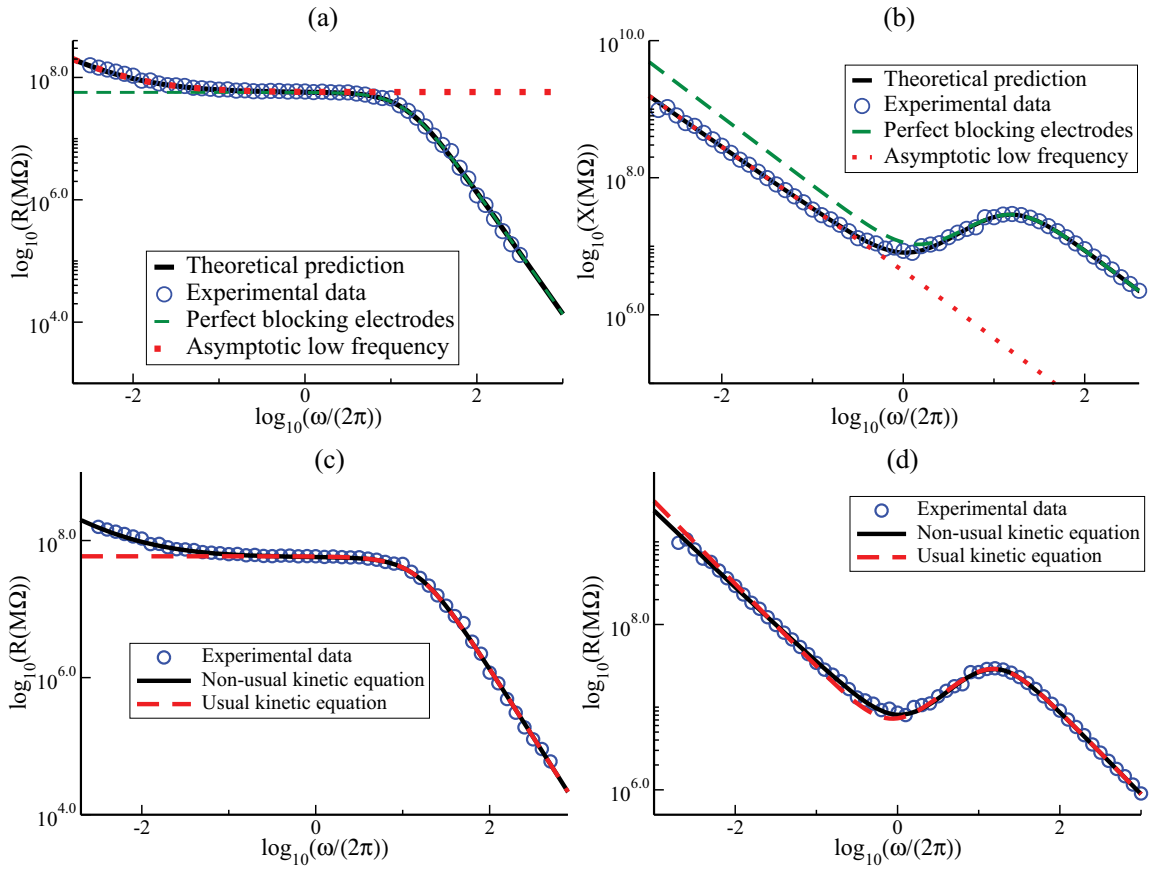

FIG. 3. (Color online) Real (a) and imaginary (b) parts of the electrical impedance of the cell vs the frequency of the applied voltage, $f = \omega/2\pi$. The parameters (in SI units) are $S = 10^{-4}$ m^2, $\varepsilon = 7.5\varepsilon_0$, $D_p = D_m = 2.5 \times 10^{-12}$ m^2/s, $d = 37 \times 10^{-6}$ m, $\kappa = 2 \times 10^{-6}$ m^3/s, $\tau = 0.12$ s, $\lambda = 1.61 \times 10^{-7}$ m, and $\gamma = 0.07$. The experimental data illustrated by the circles (blue) correspond to the sample AU10 (see the text) and the solid line (black) represents the results obtained from Eq. (34). To highlight the strengths of the model, the dotted (red) line represents the graphic made with Eq. (35), showing the importance of the surface terms in the low-frequency region. The dashed (green) curve represents the case for perfect blocking electrodes [$Z \sim 1/(i\omega)$], where the agreement is poor at low frequencies. (c) and (d) show a comparison of the experimental data (blue circles) and theoretical predictions made by using the kinetic equation, Eq. (9) (black solid line), and the usual kinetic equation (red dashed line) [17,28]. The usual kinetic equation is not capable of reproducing the experimental data at low frequencies.

times it recovers the usual, Debye-like case. For simplicity, the same parameters as in Fig. 1 were used. In the low-frequency limit, the behavior of the impedance with this choice of $K(t)$ is similar to the that reported in Refs. [44,45], which is connected to the roughness of the surfaces and their fractal characteristics. The behavior of the impedance for this case changes significantly for the real and imaginary parts in the low-frequency regime, indicating an anomalous behavior with memory effects at the surfaces.

B. Comparison with experimental results

The validation of the theoretical predictions is accomplished by confronting experimental data measured for a nematic cell with the model presented here. The liquid crystal 5CB (Merck) was used and filled into a cell prepared with Mylar spacers of 30-μ m nominal thickness. The electrode used consists of an evaporated gold pixel with surface area of 1×1 cm^2. Rubbed polyimide was used as the alignment layer for the liquid crystal, where the layer thickness used was 20 nm, achieved by spin coating the substrates with 10 wt. % solution of LQ1800 (Hitachi) in methyl pyrrolidinone (the sample is referred hereafter as AU10). The complex impedance has been measured by a Potentiostat/Galvanostat/Impedentiometer EG&G Model 273A in a frequency range from 10^{-3} to 10^5 Hz. Low amplitude of the sinusoidal applied voltage was chosen, 25 mV rms, to avoid electrically induced reorientation of the liquid crystal. One connector acts as working electrode, while the counter electrode has been short-circuited with the reference one. Measurements at lower voltages give the same results but introduce more noise. Moreover, we are further below any 5CB threshold (dielectric reorientation or flexoelectric effect) [3,4].

In Fig. 3, the experimental results obtained with the procedure discussed above are compared with the model developed in Sec. II. We used the same parameters that were used in the experiment such as cell gap, electrode area and dielectric constant. For simplicity, we neglected the combination-recombination process. At the same time, other parameters not determined in the experiment were found in the literature, such as diffusion constants and density of ions. Finally, the fit was performed by setting κ, τ, and γ as fitting parameters and by using the same kernel used in Fig. 2. The agreement between

the experimental data and the model is good, suggesting that the processes present in the surface of the electrode may be governed by a kinetic equation incorporating a non-Debye relaxation process. To further test our model, we also obtained the asymptotic expression for the impedance in the low-frequency limit to investigate how the surface effects, represented by the boundary condition, influence the dynamic of the system. By considering equal mobilities for positive and negative ions, and by treating the problem in the absence of generation and recombination terms, it is possible to demonstrate that

$$Z \sim \frac{2\lambda^2}{\epsilon i\omega S}\left(\frac{1}{\lambda + \Omega(i\omega)} + \frac{d}{2D} i\omega\right), \tag{35}$$

where $\Omega(i\omega) = \kappa\tau/\{[(i\omega\tau)^{\gamma} + K(i\omega)]\}$. This expression shows that the surfaces effects, represented by $\Omega(i\omega)$ [first term in Eq. (35)], play the decisive role in the low-frequency limit of the impedance. γ and $K(i\omega)$ are used to represent the nature of the surface phenomena, for instance, if the surface adsorbs through chemical reactions (chemisorption), physical interactions (physisorption), or both simultaneously, as discussed in Refs. [13,14]. In this sense, the experimental data is a guide of the mechanisms to perform a suitable choice to represent the process that occurs on the surface. Furthermore, it may be instructive to note that the results obtained, for example, in Refs. [17,28], by employing the usual kinetic equation, are not rich enough to reproduce the behavior of the experimental data, since in the low-frequency limit the usual kinetic equation always gives $Z \sim 1/(i\omega)$, a behavior quite different from the measured data. Figure 3(a) shows the real part of the impedance, the circles (blue) represent the experimental data, the solid line (black) is the best fit using our model, the dotted line (red) shows the asymptotic behavior given by Eq. (35), and the dashed line (green) represents the best fit of the usual model for perfect blocking electrodes. Figure 3(b) shows the imaginary part of the impedance. Figures 3(c) and 3(d) show a comparison of the experimental data (blue circles) and theoretical predictions made by using the kinetic equation, Eq. (9) (black solid line), and the usual kinetic equation (red dashed line), used in Refs. [17,28]. The usual kinetic equation is shown to be not rich enough to face the highly complex behavior of the experimental data at low frequencies.

V. CONCLUSIONS

Ionic impurities dissolved in insulating materials such as liquid crystals play an important role in the dielectric response of the medium. These ions diffuse around the cell and experience strong surface effects, such as the adsorption-desorption phenomenon. We have shown that these surface effects and the generation and recombination of ions give rise to a diffusive process that is strictly anomalous, yielding a non-Debye relaxation process, with non-usual behavior of the impedance. Due to the time scales involved in the process, it is possible to observe the role of each contribution in the impedance vs frequency curves. The agreement of the model with experimental data for a sample of 5CB liquid crystal is very good, where the encountered fitting parameters are very close to the ones used in the measurement. As a matter of fact, a model accounting for surface memory effects in the ionic dynamics brings new perspectives for non-usual behavior found in certain liquid crystal systems such as those formed by bent-core molecules and also advances comprehension about the influence of the surface roughness on the electrical response of a system described by the Poisson equation with suitable boundary conditions.

ACKNOWLEDGMENTS

This work was partially supported by the National Institutes of Science and Technology (INCT-CNPq) of Complex Systems (E.K.L.), Complex Fluids (L.R.E.), and CNPq (R.S.Z.).

[1] H. Pu, W. H. Meyer, and G. Wegner, Macromol. Chem. Phys. **202**, 1478 (2001).
[2] C. Gabriel, S. Gabriely, and E. Corthout, Phys. Med. Biol. **41**, 2231 (1996).
[3] A. Jakli and A. Saupe, *One- and Two-Dimensional Fluids* (CRC Press, Boca Raton, 2006).
[4] S.-T. Wu and D. K. Yang, *Fundamentals of Liquid Crystal Devices* (Wiley, Chichester, 2006).
[5] R. Metzler and J. Klafter, Phys. Rep. **339**, 1 (2000).
[6] R. Hilfer, *Applications of Fractional Calculus in Physics* (World Scientific, Singapore, 2000).
[7] F. Bouchet and J. Barré, J. Phys: Conf. Ser. **31**, 18 (2006).
[8] V. Latora, A. Rapisarda, and S. Ruffo, Phys. Rev. Lett. **83**, 2104 (1999).
[9] V. Latora, A. Rapisarda, and C. Tsallis, Phys. Rev. E **64**, 056134 (2001).
[10] K. G. Wang, J. Phys. A: Math. Gen. **27**, 3655 (1994).
[11] E. K. Lenzi, L. R. Evangelista, G. Barbero, and F. Mantegazza, Europhys. Lett. **85**, 28004 (2009).
[12] E. K. Lenzi, C. A. R. Yednak, and L. R. Evangelista, Phys. Rev. E **81**, 011116 (2010).
[13] R. S. Zola, E. K. Lenzi, L. R. Evangelista, and G. Barbero, Phys. Rev. E **75**, 042601 (2007).
[14] R. S. Zola, F. C. M. Freire, E. K. Lenzi, L. R. Evangelista, and G. Barbero, Chem. Phys. Lett. **438**, 144 (2007).
[15] M. A. Lomholt, I. M. Zaid, and Ralf Metzler, Phys. Rev. Lett. **98**, 200603 (2007).
[16] G. Barbero and A. L. Alexe-Ionescu, Liq. Cryst. **32**, 943 (2005).
[17] G. Barbero and L. R. Evangelista, *Adsorption Phenomena and Anchoring Energy in Nematic Liquid Crystals* (Taylor & Francis, London, 2006).
[18] J. R. Macdonald, Phys. Rev. **92**, 4 (1953).
[19] J. R. Macdonald and D. R. Franceschetti, J. Chem. Phys. **68**, 1614 (1978).
[20] D. R. Franceschetti and J. R. Macdonald, J. Appl. Phys. **50**, 291 (1979).
[21] D. R. Franceschetti and J. R. Macdonald, J. Electrochem. Soc. **129**, 1754 (1982).
[22] J. R. Macdonald, J. Electrochem. Soc. **135**, 2274 (1988).

[23] J. R. Macdonald, J. Chem. Phys. **116**, 3401 (2002).
[24] J. R. Macdonald, Phys. Rev. B **71**, 184307 (2005).
[25] J. R. Macdonald, J. Phys.: Condens. Matter **17**, 4369 (2005).
[26] J. R. Macdonald, J. Phys.: Condens. Matter **18**, 629 (2006).
[27] J. R. Macdonald, J. Phys. Chem. B **112**, 13684 (2008).
[28] J. L. de Paula, J. A. da Cruz, E. K. Lenzi, and L. R. Evangelista, J. Electroanal. Chem. **682**, 116 (2012).
[29] T. Pajkossy, J. Electroanal. Chem. **300**, 1 (1991).
[30] B. Y. Park, R. Zaouk, C. Wang, and M. J. Madou, J. Electrochem. Soc. **154**, P1 (2007).
[31] B. Sapoval, in *Fractals and Disordered Systems*, edited by A. Bunde and S. Havlin (Springer-Verlag, Berlin, 1996), Chap. 6, pp. 233–261.
[32] G. Barbero, Phys. Rev. E **71**, 062201 (2005).
[33] G. Barbero, M. Becchi, A. Strigazzi, J. LeDigabel, and A. M. Figueiredo Neto, J. Appl. Phys. **101**, 044102 (2007).
[34] F. Batalioto, O. G. Martins, A. R. Duarte, and A. M. Figueiredo Neto, Eur. Phys. J. E **34**, 10 (2011).
[35] E. K. Lenzi, L. R. Evangelista, and G. Barbero, J. Phys. Chem. B **113**, 11371 (2009).
[36] F. Ciuchi, A. Mazzulla, N. Scaramuzza, E. K. Lenzi, and L. R. Evangelista, J. Phys. Chem. C **116**, 8773 (2012).
[37] J. R. Macdonald, L. R. Evangelista, E. K. Lenzi, and G. Barbero, J. Phys. Chem. C **115**, 7648 (2011).
[38] P. A. Santoro, J. L. de Paula, E. K. Lenzi, and L. R. Evangelista, J. Chem. Phys. **135**, 114704 (2011).
[39] J. Bisquert and A. Compte, J. Electroanal. Chem. **499**, 112 (2001).
[40] J. Bisquert, G. Garcia-Belmonte, and A. Pitarch, Chem. Phys. Chem. **4**, 287 (2003).
[41] J. Bisquert, Phys. Rev. E **72**, 011109 (2005).
[42] J. Bisquert, Phys. Rev. Lett. **91**, 010602 (2003).
[43] G. Barbero and L. R. Evangelista, Phys. Rev. E **70**, 031605 (2004).
[44] T. C. Halsey and M. Leibic, Ann. Phys. **219**, 109 (1992).
[45] L. Nyikos and T. Pajkossy, Electrochim. Acta **30**, 1533 (1985).
[46] J. B. Bates, Y. T. Chu, and W. T. Stribling, Phys. Rev. Lett. **60**, 627 (1988).
[47] A. Le Mehaute and G. Crepy, Solid State Ionics **9-10**, 17 (1983).
[48] G. Derfel, E. K. Lenzi, C. R. Yednak, and G. Barbero, J. Chem. Phys. **132**, 224901 (2010).
[49] P. Salamon, N. Éber, Á. Buka, J. T. Gleeson, S. Sprunt, and A. Jákli, Phys. Rev. E **81**, 031711 (2010).
[50] A. Jákli, D. Krüerke, and G. G. Nair, Phys. Rev. E **67**, 051702 (2003).
[51] R. Gorenflo and F. Mainardi, in *Fractals and Fractional Calculus in Continuum Mechanics*, edited by A. Carpinteri and F. Mainardi, Vol. 378 Series CISM Courses and Lecture Notes (Springer-Verlag, Wien, 1997), pp. 223–276.